View metadata, citation and similar papers at core.ac.uk
brought to you by CORE
provided by Scholarly Materials And Research @ Georgia Tech

Proceedings of the 29th Annual International Conference of the IEEE EMBS
Cité Internationale, Lyon, France
August 23-26, 2007.

Computational Modeling of A Metabolic Pathway in Ceramide *de novo* Synthesis

Shobhika Dhingra, Melissa Freedenberg, Chang F Quo, Alfred H. Merrill Jr., May D Wang

Abstract— Studies have implicated ceramide as a key molecular agent in regulating programmed cell death, or apoptosis. Consequently, there is significant potential in targeting intracellular ceramide as a cancer therapeutic agent. The cell's major ceramide source is the ceramide *de novo* synthesis pathway, which consists of a complex network of interdependent enzyme-catalyzed biochemical reactions. To understand how ceramide works, we have initiated the study of the ceramide *de novo* synthesis pathway using computational modeling based on fundamental principles of biochemical kinetics. Specifically, we designed and developed the model in MATLAB SIMULINK for the behavior of dihydroceramide desaturase. Dihydroceramide desaturase is one of three key enzymes in the ceramide *de novo* synthesis pathway, and it converts a relatively inert precursor molecule, dihydroceramide into biochemically reactive ceramide. A major issue in modeling is parameter estimation. We solved this problem by adopting a heuristic strategy based on *a priori* knowledge from literature and experimental data. We evaluated model accuracy by comparing the model prediction results with interpolated experimental data. Our future work includes more experimental validation of the model, dynamic rate constants assessment, and expansion of the model to include additional enzymes in the ceramide *de novo* synthesis pathway.

I. Introduction

Ceramide is implicated in cell apoptosis, making it a viable candidate for cancer research [1]. The ceramide *de novo* synthesis pathway is a major source of ceramide in the cell. Building a model to describe ceramide *de novo* synthesis pathway will facilitate experimental scientists to optimize experimental design in the lab. In the long term, it will help predict the effects of a particular drug on the ceramide *de novo* synthesis pathway, and improve disease prognosis and treatment as a form of patient-customized medicine.

Manuscript received April 16, 2007. This research has been supported by grants from National Institutes of Health (Bioengineering Research Partnership R01CA108468, Center for Cancer Nanotechnology Excellence U54CA119338), Georgia Cancer Coalition (Distinguished Cancer Scholar Award to Professor Wang) and Microsoft Research.

S. Dhingra, M. Freedenberg and C. Quo are with the Wallace H. Coulter Department of Biomedical Engineering, Georgia Institute of Technology and Emory University, Atlanta, GA 30332 USA (emails: {gtg225q, gtg415g, gtg801f} @mail.gatech.edu).

A H Merrill, Jr. is with the School of Biology, Georgia Institute of Technology, Atlanta, GA 30332 USA (email: al.merrill@biology.gatech.edu).

May D. Wang (corresponding author) is with the Wallace H. Coulter Department of Biomedical Engineering, Georgia Institute of Technology and Emory University, Atlanta, GA 30332 USA (phone: (404) 385-2954, e-mail: maywang@bme.gatech.edu).

II. Biological Motivation

Ceramide is a sphingolipid that plays a key role in apoptosis, or programmed cell death [1, 2]. Ceramide is generated from one of two major pathways: (a) ceramide catabolism from molecules such as sphingomyelin and (b) the ceramide *de novo* synthesis pathway, which produces ceramide from serine and palmitoyl-coA. Production of certain ceramides, such as those with a length 16 fatty acyl chain (ceramide-16) [3], is known to increase cytotoxicity. Intracellular metabolic response to external stimuli such as heat shock and exposure to chemotherapy have been associated with increased levels of pro-apoptotic ceramides [4, 5]. As such, ceramide has the potential to provide selective toxicity to malignant cells, and is a potentially significant target for cancer research [1-2, 4-6]. Thus, understanding the dynamics of the ceramide *de novo* synthesis pathway is imperative for unleashing its cancer-fighting power.

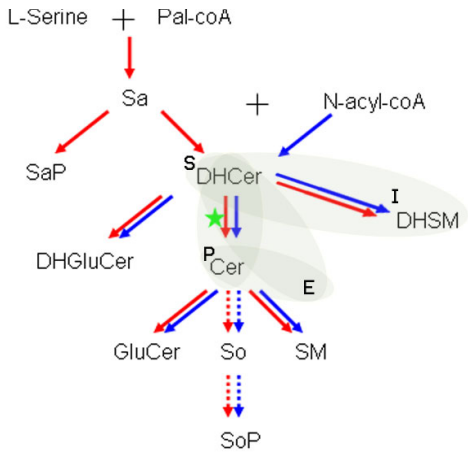

Figure 1. Digram of ceramide *de novo* synthesis pathway. "Star" labels reactions that are catalyzed by the enzyme dihydroceramide desaturase. "E" denotes "dihydroceramide desaturase".

III. Methods

A. Modeling the ceramide de novo synthesis pathway

For this study, we focused on one specific reaction in the ceramide *de novo* synthesis pathway, the desaturation reaction of dihydroceramide-16 (DHCer) into ceramide-16 (Cer) that is catalyzed by the enzyme dihydroceramide

desaturase. This specific reaction is highlighted in the pathway shown in Figure 1.

B. Michaelis-Menten & the King-Altman algorithm

The triangular-form mechanism shown in Figure 2 was constructed using Michaelis-Menten kinetics combined with the King-Altman algorithm[7,8]. DHCer is designated as substrate (S), Cer is designated as product (P), and dihydrosphingomyelin (DHSM) is designated as inhibitor (I). DHSM was assumed to be the sole inhibitor of the reaction based on the structural similarity between DHSM and DHCer, especially with regards to the size of the functional head-group[9].

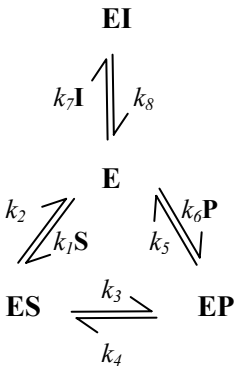

Figure 2. King-Altman geometric representation of an enzymatic reaction model with competitive inhibition. S = substrate DHCer, P = product, Cer, and I = inhibitor DHSM, ES = enzyme-substrate complex, EP = enzyme-product complex, EI = enzyme-inhibitor complex, k_i's = rate constants

Based on Figure 2, reaction rate equations 1-4 were derived as follows, where, E_o = total enzyme concentration, and $\Sigma = (([E] + [ES] + [EI] + [E]) / E_o)$:

$$\frac{[E]}{[E_o]} = \frac{k_2k_4k_8 + k_3k_5k_8 + k_2k_5k_8}{\Sigma} \quad (1)$$

$$\frac{[ES]}{[E_o]} = \frac{k_1k_4k_8S + k_1k_5k_8S + k_4k_6k_8P}{\Sigma} \quad (2)$$

$$\frac{[EP]}{[E_o]} = \frac{k_1k_3k_8S + k_3k_6k_8P + k_2k_6k_8P}{\Sigma} \quad (3)$$

$$\frac{[EI]}{[E_o]} = \frac{k_2k_4k_7I + k_3k_5k_7I + k_2k_5k_7I}{\Sigma} \quad (4)$$

Equations 5-7 were then derived from Figure 2 to describe the rates of change of substrate [S], product [P] and inhibitor [I] concentrations:

$$\frac{d[S]}{dt} = k_2[ES] - k_1[E][S] \quad (5)$$

$$\frac{d[P]}{dt} = k_5[EP] - k_6[E][P] \quad (6)$$

$$\frac{d[I]}{dt} = k_8[EI] - k_7[E][I] \quad (7)$$

Equations 1-4 were then substituted into equations 5-7, yielding equations 8-10. This was a necessary because concentrations of ES, EP, and EI intermediates are not known.

$$\frac{d[S]}{dt} = \frac{k_2k_4k_6k_8[P] - k_1k_3k_5k_8[S]}{\Sigma}[E_o] \quad (8)$$

$$\frac{d[P]}{dt} = \frac{k_1k_3k_5k_8[S] - k_2k_4k_6k_8[P]}{\Sigma}[E_o] \quad (9)$$

$$\frac{d[I]}{dt} = 0 \quad (10)$$

C. Experimental Data Acquisition

In vivo data on ceramide concentration dynamics was obtained over six hours at one hour intervals by the Georgia Tech Sphingolipid Research Laboratory using LC-MS/MS mass spectrometry. This data is the basis for initial model conditions listed in Table I. Cubic spline interpolation was performed on the mass spectrometry data to establish a basis for model validation.

D. Parameter Estimation

Table II summarizes physical embodiments of the model rate constants, the values which were chosen to model them, and the basis for their choice. k_3 and k_6, were chosen based on *a priori* knowledge, and the remainder of constants were chosen based on physical assumptions.

E. Simulation

Equations 8-10 were implemented in Matlab Simulink as shown in Figure 3 using initial conditions from Table I and parameter values from Table II. Product and substrate concentrations were tracked over a period of simulation-time units equivalent to six hours real-time.

Table I. Model initial conditions

Biological Species	Initial Concentration (pmol/mg protein)
Ceramide (Cer)	98.340000000E-12
Dihydroceramide (DHCer)	4.630417394E-11
Dihydrospingomyelin (DHSM)	1.927537263E-7

IV. RESULTS

Cubic spline interpolated mass spectrometry data was graphically overlaid on simulation results, as shown in Figure 4. The simulation predicted a linear increase in Cer

concentration with time (trend unobserved at presented scale) and a much faster concurrent linear decrease in DHCer concentration. Interpolated experimental data, represented by the dotted line in Figure 4, revealed that, in general, Cer concentration does actually increase with time but at a nonlinear rate.

Table II. Physical embodiments & basis for estimation of rate constants

Rate Constant	Physical Embodiment	Value(s^{-1})	Basis for Value Estimation
k_1	Formation of enzyme-substrate complex by substrate recruitment of free enzyme; involves forming weak valence chemical bonds	10E-5	Formation of the enzyme-substrate complex from free enzyme and substrate molecules with weak valence chemical bonds is much easier than formation and breakage of strong covalent chemical bonds as in k_3 i.e. $k_1 >> k_3$.
k_2	Formation of free enzyme by substrate release from enzyme-substrate complex; involves breaking weak valence chemical bonds	10E-6	Release of substrate from enzyme-substrate complex is similar to, but occurs less readily than, association of free enzyme and substrate molecules in k_1.
k_3	Formation of enzyme-product complex from enzyme-substrate complex; involves breaking and forming strong covalent chemical bonds	17.8E-9	Obtained from literature [2] i.e. seed parameter from experimental validation; this is used as point of reference for estimating other k_i's.
k_4	Formation of enzyme-product complex from enzyme-substrate complex; involves breaking and forming strong covalent chemical bonds	10E-13	Backward reaction of enzyme-substrate complex formation from enzyme-product complex is much smaller than forward reaction in order for overall pathway to proceed forward i.e. $k_4 << k_3$.
k_5	Formation of free enzyme by product release from enzyme-product complex; involves breaking weak valence chemical bonds	10E-4	Release of product from enzyme-product complex is similar to, but occurs more readily than, association of free enzyme and substrate molecules in k_1.
k_6	Formation of the enzyme-product complex; involves forming weak valence chemical bonds	0	Formation of enzyme-product complex from free enzyme and product molecules is negligible based on classical Michaelis-Menten assumptions; may also be interpreted as consequence of enzyme specificity.
k_7	Formation of the enzyme-inhibitor complex; involves forming weak valence chemical bonds	10E-7	The competitive inhibition model assumes reversible binding of free enzyme and inhibitor molecules that involves weak valence chemical bonds; enzyme-inhibitor affinity is a function of molecular similarity between substrate and inhibitor molecules. Here, enzyme-inhibitor affinity is considered to be less than enzyme-substrate affinity i.e. $k_7 < k_1$.
k_8	Formation of free enzyme by inhibitor release; involves breaking weak valence chemical bonds	10E-7	Dissociation of enzyme-inhibitor complex assumed to occur at same rate as association.
E_o	Total enzyme concentration	10E-7	By Michaelis-Menten assumptions, enzyme is saturated, so this value should be >> Cer and DHCer from Table 1.

V. DISCUSSION

There is a considerable disparity between interpolated Cer experimental data and the simulation results derived from classical Michaelis-Menten kinetics. Simulation results do agree with the physical expectation that in an enzymatic system, the concentration of substrate and product over time are related by an inverse trend. However, additional experimental data (not presented) indicated that DHCer undergoes an initial decrease followed by a steady increase after 3 hours real-time later, which is not shown by simulation; the nonlinear dynamics of the interpolated experimental data are not mirrored in the simulated results.

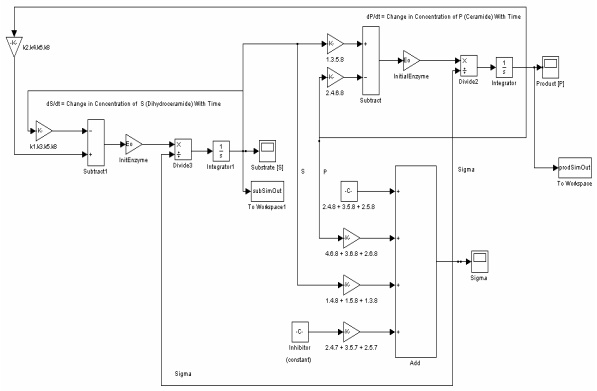

Figure 3. Simulink implementation of system equations.

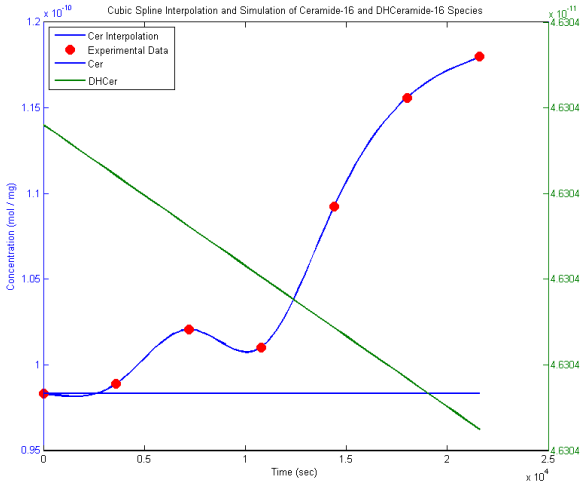

Figure 4. Cubic Spline Interpolation and Simulation of Ceramide-16 and DHCeramide-16 species. Left-hand (Ceramide) axis is on the scale of (0.95 to 1.2)E-10 pmol/mg. Right-hand (DHCeramide) axis is on the scale of 4.604E-11 pmol/mg. X-axis (seconds) is on the scale of 0 to 2.5E4 seconds.

As such, the classical Michaelis-Menten linear model explored in this study does not sufficiently simulate the dynamic reactions of DHCer and Cer in the ceramide *de novo* synthesis pathway catalyzed by the enzyme dihydroceramide desaturase.

Parameter estimation is one major issue in this study. Model parameters, specifically reaction rate constants $\{k_i$'s$\}$ and total enzyme concentration $[E_o]$, were estimated based on limited numerical data from literature reviews and basic biochemical assumptions. Reaction rates were assumed constant throughout the simulation. However, reaction rates in the ceramide *de novo* synthesis pathway have been shown to slowly change with time by Hanada [10]. Ideally, a set of dynamic rate values should be derived for the model to maximize its consistent accuracy with time. Because parameter values are not exact, a sensitivity analysis must be performed to identify which rate constants are most important for governing system behavior. It is expected that k_3, the rate of conversion of the enzyme-substrate [ES] to the enzyme-product [EP] complex, will be most sensitive to perturbation, while the rate constant for the reverse reaction, k_4, will be the least sensitive to ensure that the transition from substrate to product proceeds forward.

Another limitation is the assumption that DHSM was the sole inhibitor of the dihydroceramide desaturase reaction. In reality, more molecules also inhibit this reaction, and their consideration may be necessary to create an accurate model. In addition, there is some anecdotal evidence that dihydroceramide desaturase acts on multiple molecules containing an unsaturated C-C bond [10-13]. Due to this the fundamental Michaelis-Menten assumption that dihydroceramide desaturase is saturated with DHCer and Cer may be violated.

While the model developed herein is not perfect, it is a viable starting point for modeling the action of dihydroceramide desaturase. Once this model is perfected, it may be adapted directly to modeling other enzymes in the ceramide *de novo* synthesis pathway, and finally the models of each enzyme may be combined to create a complete pathway model.

ACKNOWLEDGMENT

The authors wish to thank Christopher Haynes and Jeremy Allegood for high-resolution time-series mass spectrometry data and valuable discussions, especially with regard to the ceramide *de novo* synthesis pathway.

REFERENCES

[1] Reynolds P C, Maurer B J, and Kolesnick R N. "Ceramide synthesis and metabolism as a target for cancer therapy." Cancer Letters. 2003 Aug 13; 206: 169–180.
[2] Christoph M, et al. "Characterization of ceramide synthesis." J Biol Chem. 1997; 272(36): 22432-22437.
[3] Maceyka, M. et al. "SphK1 and SphK2, Sphingosine Kinase Isoenzymes with Opposing Functions in Sphingolipid Metabolism." J. Biol Chemistry (2005). 280;37118-37129.
[4] Wells, G, Dickson, R, Lester, R. "Heat-induced elevation of ceramide in saccharomyces cerevisiae via de novo synthesis." J Biol Chem. 1998; 273: 7235-7243.
[5] Jenkins, G M, Coward, A, Signorelli, P, Pettus B J, Chalfant, C E, Hannun, Y A. "Acute activation of the de novo sphingolipid biosynthesis upon heat shock causes an accumulation of ceramide and subsequent dephosphorylation of SR proteins." J Biol Chem. 2002; 277: 42572-42578.
[6] Riebeling, C, Allegood, J C, Wang, E, Merrill, A H, Futerman, A H. "Two mammalian longevity assurance gene (LAG1) family members, trh1 and trh4, regulate dihydroceramide synthesis using different fatty acyl-coA donors." J Biol Chem. 2003; 278: 43452-43459.
[7] King, E L, and Altman, C. "A schematic method of deriving the rate laws for enzyme-catalyzed reactions." Jour Amer Chem Soc. 1956; 60: 1375-1378.
[8] D. Voet, J.G. Voet, and C. W. Pratt, Fundamentals of Biochemistry, New York: Wiley, 1999.
[9] "Lipid Maps." 1 Jun 2007 <http://www.lipidmaps.org>.
[10] Hanada, K. "Serine palmitoyltransferase, a key enzyme of sphingolipid metabolism." Biochimica et Biophysica Acta. 2003; 1632: 16-30.
[11] Pewzner-Jung, Y, Ben-Dor, S, and Futerman, A. "When do Lasses (longevity assurance genes) become CerS (ceramide synthases)." J Biol Chem. 2006; 281: 25001-25005.
[12] Schulz, A et al. "The CLN9 protein, a regulator of dihydroceramide synthase." J Biol Chem. 2006; 281: 2784-2794.
[13] Maceyka, M et al. "SphK1 and SphK2, sphingosine kinase isoenzymes with opposing functions in sphingolipid metabolism." J Biol Chem. 2005; 280: 37118-37129.
[14] Ma L, and Iglesias, P A. "Quantifying robustness of biochemical network models." BMC Bioinformatics. 2002; 3: 38.
[15] van Riel N A W. "Dynamic modeling and analysis of biochemical networks: mechanism-based models and model-based experiments." Briefings in Bioinformatics. 2006; 7(4): 364-374.